

# Vascular endothelial growth factor immobilized in collagen scaffold promotes penetration and proliferation of endothelial cells

Yi Hao Shen<sup>a</sup>, Molly S. Shoichet<sup>a,b,c,d</sup>, Milica Radisic<sup>a,b,e,\*</sup>

<sup>a</sup> Institute of Biomaterials and Biomedical Engineering, University of Toronto, 164 College Street, Rm. 407, Toronto, Ontario, Canada M5S 3G9

<sup>b</sup> Department of Chemical Engineering and Applied Chemistry, University of Toronto, Ontario, Canada

<sup>c</sup> Terrence Donnelly Centre for Cellular and Biomolecular Research, University of Toronto, Toronto, Ontario, Canada

<sup>d</sup> Department of Chemistry, University of Toronto, Toronto, Ontario, Canada

<sup>e</sup> Heart and Stroke/Richard Lewar Centre of Excellence, University of Toronto, Toronto, Ontario, Canada

Received 10 August 2007; received in revised form 20 November 2007; accepted 18 December 2007

Available online 5 February 2008

## Abstract

A key challenge in engineering functional tissues *in vitro* is the limited transport capacity of oxygen and nutrients into the tissue. Inducing vascularization within engineered tissues is a key strategy to improving their survival *in vitro* and *in vivo*. The presence of vascular endothelial growth factor (VEGF) in a three-dimensional porous collagen scaffold may provide a useful strategy to promote vascularization of the engineered tissue in a controlled manner. To this end, we investigated whether immobilized VEGF could promote the invasion and assembly of endothelial cells (ECs) into the collagen scaffolds. We conjugated VEGF onto collagen scaffolds using *N*-(3-dimethylamino-propyl)-*N'*-ethylcarbodiimide hydrochloride chemistry, and measured the concentrations of immobilized VEGF in collagen scaffolds by direct VEGF enzyme-linked immunosorbent assay. We demonstrated that immobilized VEGF (relative to soluble VEGF) promoted the penetration and proliferation of ECs in the collagen scaffold, based on results of cell density analysis in histological sections, immunohistochemistry, XTT proliferation assay, glucose consumption and lactate production. Furthermore, we observed increased viability of ECs cultured in scaffolds with immobilized VEGF relative to soluble VEGF. This research demonstrates that immobilization of VEGF is a useful strategy to promote the invasion and proliferation of ECs into a scaffold, which may in turn lead to a vascularized scaffold.

© 2008 Acta Materialia Inc. Published by Elsevier Ltd. All rights reserved.

**Keywords:** Collagen scaffold; Endothelial cell; VEGF; Covalent immobilization; Tissue engineering

## 1. Introduction

One of the main goals of tissue engineering is to design tissue scaffolds that can support the survival, growth and assembly of cells into functional tissues. A key challenge in engineering functional tissues is the limited transport capacity of oxygen and nutrients into the tissue. For example, in hypoxia-sensitive cardiac tissue engineered *in vitro*, conven-

tional medium diffusion can provide oxygen at a distance of up to 100  $\mu\text{m}$ , yet oxygen transport beyond this distance is limited [1,2]. As a result, the interior of a cardiac construct has low cell density and viability [3,4]. Oxygen gradients were shown to correlate with cell density and cell viability in engineered cardiac constructs [5].

Inducing vascularization is a key strategy to improving the survival of engineered tissues both *in vitro* and *in vivo* [6,7]. The most studied approach is the delivery of angiogenic growth factors to promote neovascularization [8]. Vascular endothelial growth factor (VEGF) is a potent inducer of endothelial cell (EC) proliferation, migration and tube formation, and is a key mediator in the process of angiogenesis [8,9]. There exist a family of VEGFs,

\* Corresponding author. Address: Institute of Biomaterials and Biomedical Engineering, University of Toronto, 164 College Street, Rm. 407, Toronto, Ontario, Canada M5S 3G9. Tel.: +1 416 946 5295; fax: +1 416 978 4317.

E-mail address: [m.radisic@utoronto.ca](mailto:m.radisic@utoronto.ca) (M. Radisic).

VEGF-A through VEGF-E, of which an isoform of VEGF-A, VEGF<sub>165</sub>, is the most prevalent [8]. Two distinct VEGF receptor tyrosine kinases, VEGFR-1 (flt-1) and VEGFR-2 (KDR/flk-1), have been identified on ECs [10–12]. It is thought that flk-1 functions in inducing EC proliferation, while flt-1 functions in differentiation and vascular organization [11]. Binding of VEGF to VEGF receptor leads to receptor dimerization and autophosphorylation, which allows for the recruitment of signaling proteins containing src-homology-2 (SH2) domains to specific phosphorylated tyrosines [11].

There has been tremendous success in using biomaterials for the controlled delivery of VEGF to induce neovascularization [13–16], as well as to support cell survival and differentiation [17–19]. Alternately, growth factors such as VEGF can be immobilized onto the biomaterial scaffolds for tissue engineering applications. Immobilized growth factors can promote the desired cell-material interactions, and render synthetic materials bioactive [20,21]. Several studies have shown enhanced proliferation of ECs on two-dimensional substrates with immobilized VEGF. Taguchi and colleagues immobilized VEGF onto poly(acrylic acid) grafted poly(ethylene) films using *N*-(3-dimethylaminopropyl)-*N'*-ethylcarbodiimide hydrochloride (EDC) chemistry, and found that VEGF and fibronectin co-immobilized surface greatly promoted the growth of human umbilical vein endothelial cells (HUVECs) [22]. Ito and colleagues photo-immobilized VEGF onto gelatin surfaces, and showed that immobilized VEGF greatly enhanced the proliferation and surface coverage of HUVECs [23]. Backer and colleagues engineered a cysteine tag into VEGF and then conjugated VEGF onto fibronectin-coated surfaces via the cysteine tag, and observed growth stimulation of VEGFR-2 over-expressing cells [24]. Zisch and colleagues engineered a Factor XIIIa substrate sequence into VEGF and crosslinked VEGF into the fibrin gel through a coagulation process, and subsequently demonstrated growth enhancement of HUVECs cultured on VEGF–fibrin surfaces [25].

The main objective of this work was to immobilize VEGF into a porous three-dimensional (3D) collagen scaffold to promote the penetration and assembly of ECs into the scaffold. We chose to use porous collagen scaffolds because they are widely used in tissue engineering to support the growth of various cell types, and are also used for surgical wound dressings. We demonstrated that VEGF maintained biological activity upon immobilization and promoted the infiltration and proliferation of ECs in the 3D collagen scaffold. This research is the first step in assembling a high density of ECs in a 3D scaffold, in order to promote vascularization within the engineered tissue constructs.

## 2. Materials and methods

### 2.1. Collagen scaffolds

Scaffolds were discs (7 mm diameter × 2 mm thick) punched from sheets of commercially available Ultra-

foam™ collagen hemostat (Davol Inc., Cranston, RI). According to the manufacturer's specifications, Ultrafoam™ is a water-insoluble, partial HCl salt of purified bovine dermal (corium) collagen formed as a sponge with interconnected pores. Dry collagen scaffold was cross-sectioned using a sharp razor balder, sputter coated with gold and imaged in face and cross-section using a Hitachi S-3400N variable pressure scanning electron microscope.

To assess the level of collagen scaffold degradation in the culture medium, the scaffolds ( $n = 3$  per group per time point) were placed in a 12-well plate and maintained in 1 ml of D4T cell culture medium for 10 min, 7 days and 12 days. Culture medium was changed by 100% every other day. The samples were immersed in distilled water for 10 min before being freeze dried in liquid nitrogen for 10 min. The samples were then placed into the lyophilizer for 24 h to dry under vacuum followed by measurements of dry weight.

### 2.2. Immobilization of VEGF in collagen scaffold

Mouse recombinant VEGF<sub>165</sub> was immobilized into the porous collagen scaffold using EDC chemistry. The collagen scaffold (7 mm diameter, 2 mm thickness, cut out from the collagen sponge sheet using a circular metal borer) was immersed in 150  $\mu$ l of EDC (Sigma) and *N*-hydroxysulfosuccinimide (sulfo-NHS) (Pierce Chemicals) (EDC/sulfo-NHS concentrations of 24 mg/60 mg ml<sup>-1</sup> or 4.8 mg/12 mg ml<sup>-1</sup>) dissolved in PBS (filter sterilized for cell culture) in a 96-well plate. The reaction proceeded for 20 min at room temperature. The scaffold was then removed from the EDC/sulfo-NHS soaking solution and immersed completely in 100  $\mu$ l of VEGF (concentrations of 500 ng ml<sup>-1</sup> or 1  $\mu$ g ml<sup>-1</sup>) dissolved in phosphate-buffered saline (PBS). The reaction proceeded for 1 h at room temperature. The scaffold was then subjected to successive soaks in fresh PBS (eight washes of at least 5 min each) to remove any uncrosslinked VEGF and EDC/sulfo-NHS.

### 2.3. Quantification of immobilized VEGF

The amount of immobilized VEGF throughout the depth of the scaffold ( $n = 3$ ) was quantified by a direct VEGF enzyme-linked immunosorbent assay (ELISA) (BioVision VEGF ELISA kit) technique, in which the standard VEGF ELISA procedure in the kit was followed using the scaffold as the primary substance. Briefly, the scaffold was blocked in 1% bovine serum albumin (BSA) in PBS for 1 h in a 96-well plate at room temperature, after which it was washed (1% Tween-20 in PBS) for 1 min. The scaffold was then immersed in biotinylated anti-mVEGF detection antibody (0.025  $\mu$ g ml<sup>-1</sup>) in diluent (0.05% Tween-20, 0.1% BSA in PBS) for 1 h at 37 °C, after which it was washed repeatedly (six washes of at least 3 min each on a shaker). The scaffold was immersed in Avidin peroxidase conjugate (0.05% in diluent) for 30 min at room temperature, after which it was washed repeatedly. The wet scaffolds were placed in a

cryostat, frozen at  $-20^{\circ}\text{C}$  for 5–10 min and then cryosectioned into  $200\ \mu\text{m}$  thick slices, which were positioned at the bottom of the wells in a 96-well plate. Finally, 2,2'-azino-bis(3-ethylbenzothiazoline-6-sulfonic acid) liquid substrate was added to each well and color development was monitored concurrently with a series of soluble VEGF standards. Sandwich ELISA was performed concurrently with the corresponding part of the direct ELISA in order to create a standard curve for quantification of immobilized VEGF. After 20 min, the colored substrate solution was removed from each well and put into a new plate, and the absorbance was measured at 405 nm using an ultraviolet (UV) plate reader along with the standards.

#### 2.4. Cell culture

D4T, a mouse embryonic stem cell-derived endothelial cell line [26] (passage number between 15 and 25) was cultured for 1 week in scaffolds with different amounts of immobilized VEGF, unmodified scaffolds, and unmodified scaffolds with culture medium containing  $100\ \text{ng}\ \text{ml}^{-1}$  soluble VEGF. Prior to cell seeding, the scaffolds were soaked in warm culture medium, dabbed gently on sterile paper (autoclaved Kim-wipes) to remove excess moisture and placed in a 24-well plate. Cell pellet was suspended in culture medium and  $30\ \mu\text{l}$  of cell suspension containing 50,000 cells were pipetted on top of each scaffold. The plate was incubated at  $37^{\circ}\text{C}$  for 40 min for cells to attach before  $600\ \mu\text{l}$  of culture medium was added into each well. D4T culture medium contained 94% Iscove's modified Dulbecco's medium (Gibco), 5% fetal bovine serum (Gibco) and 1% penicillin/streptomycin (Gibco); the medium was changed by 100% every 2–3 days during the 1 week culture.

#### 2.5. Cell density analysis

To determine the spatial cell density immediately after seeding, the cell-seeded scaffolds were fixed in 4% paraformaldehyde for 1 h at room temperature and then immersed in a cryopreservation solution of 30% sucrose in PBS overnight. The scaffolds were then cut in half through the center, so that the cross-section at the centre of the sample was revealed. The cross-section of each sample was then placed face down in a cryomould with OCT and snap frozen with liquid nitrogen. The samples were stored at  $-80^{\circ}\text{C}$  prior to cryosectioning at  $-22^{\circ}\text{C}$  at a thickness of  $10\ \mu\text{m}$  and with an interval of  $200\ \mu\text{m}$ , so that slices of the sample cross-section were obtained. The slices were mounted with 4',6-diamidino-2-phenylindole (DAPI) mounting medium (Vector Labs) and fluorescence images (Olympus, IX81) were taken at  $\times 40$  magnification.

At the end of 1 week culture, the scaffolds were fixed as described above, immersed in 30% sucrose solution overnight and then snap frozen prior to cryosectioning. Horizontal face sections of  $10\ \mu\text{m}$  thickness were sliced starting from the top surface of the scaffold, at an interval of every  $200\ \mu\text{m}$ , along the depth of the scaffold. To analyze

cell density, the slides were mounted with DAPI mounting medium, and imaged with a fluorescence microscope at  $\times 200$  magnification. For each sample ( $n = 3$  per group) at a particular depth, two sections were imaged with three representative images taken across each section. The cell number in each image was obtained by image analysis using Image J software. Briefly, a threshold in color intensity was set for the blue channel of the image to include all DAPI-stained nuclei while excluding any background fluorescence. The "analyze particle" function was then used to count the number of nuclei in the image.

#### 2.6. CD31 immunohistochemistry

Sample sections were blocked in 10% normal horse serum (Vector Labs) in PBS for 40 min in a humidified chamber at room temperature. Rat anti-mouse CD31 primary antibody (BD Pharminogen) was applied at a dilution of 1:100 (with 1.5% serum and 0.5% Tween-20 in PBS) to the sample and incubated overnight at  $4^{\circ}\text{C}$ . The sample was washed three times in PBS, after which the fluorescein isothiocyanate-conjugated goat anti-rat secondary antibody (Sigma) was applied at a dilution of 1:100 (with 1.5% serum and 0.5% Tween-20 in PBS) to the sample and incubated at room temperature for 1 h. The sample was washed three times in PBS, after which it was mounted with DAPI mounting medium (Vector Labs). For each sample at a particular depth, representative fluorescence images were taken at  $\times 200$  magnification across two sections.

#### 2.7. XTT cell proliferation assay

The XTT assay is based on the cleavage of the yellow tetrazolium salt XTT to form an orange formazan dye by metabolic active cells. After 1 week of culture, the scaffolds ( $n = 3$  per group) were placed in a 96-well plate with  $100\ \mu\text{l}$  of culture medium added to each well. XTT assay was performed following the manufacturer's protocol (Roche Diagnostics). Briefly,  $50\ \mu\text{l}$  of XTT labeling mixture was added to each well containing the scaffold immersed in  $100\ \mu\text{l}$  of culture medium. The plate was incubated at  $37^{\circ}\text{C}$  on a shaker (30 RPM) for 2 h. Then  $100\ \mu\text{l}$  of supernatant was pipetted from each well and put into a new plate. The absorbance was measured at 450 nm using a UV plate reader. We also seeded a standard series of known number of cells into scaffolds ( $n = 2$ ), and performed XTT assay on this series of standards concurrently with the experimental samples. This allowed us to create a standard curve, and thus convert the absorbance readings into cell numbers.

#### 2.8. Glucose and lactate assays

The concentrations of glucose and lactate in culture medium were measured using colorimetric glucose (Bioassay Systems) and lactate (University of Buffalo Biomedical Research Service Center) assay kits, following the given protocols. When medium was changed during the 1 week

culture ( $n = 3$  per group), old medium supernatant was collected and stored at  $-20^{\circ}\text{C}$ .

Glucose assay is based on the formation of a colored complex between an aldohexose and *o*-toluidine-glacial acetic acid. Briefly, diluted medium samples and a series of glucose standards were mixed with assay reagent in Eppendorf tubes and heated in a boiling water bath, followed by cooling in a cold water bath. Colored product solution from each tube was transferred in duplicate into a 96-well plate, and the absorbance was measured at 630 nm using a UV plate reader.

Lactate assay is based on the reduction of the tetrazolium salt INT in an NADH-coupled enzymatic reaction to formazan color product. Briefly, diluted medium samples and a series of lactate standards were pipetted into a 96-well plate. The assay solution was added to each well and the plate was incubated at  $37^{\circ}\text{C}$  for 40 min. The reaction was stopped by adding 0.5 M acetic acid to each well, then the absorbance was measured at 492 nm using a UV plate reader.

### 2.9. Cell viability analysis

After 1 week of culture, the viability of cells in scaffolds ( $n = 3$  per group) was measured by ethidium monoazide bromide (EMA) labeling followed by fluorescent-activated cell sorting (FACS) as described by Radisic and colleagues [3]. EMA diffuses into dead cells and covalently binds to the DNA upon photolysis, thereby fluorescently labeling the DNA in dead cells. In a 96-well plate, each scaffold was immersed with  $50\ \mu\text{l}$  of EMA (Molecular Probes,  $5\ \mu\text{g}\ \text{ml}^{-1}$  in PBS). As a positive control,  $50\ \mu\text{l}$  of cell suspension (collected from the tissue culture flask) was mixed with  $50\ \mu\text{l}$  of EMA in a well. The plate was placed under a fluorescent light at a distance of 18 cm for 10 min for EMA to crosslink to the DNA of non-viable cells. The scaffolds were washed in PBS several times to rid off uncrosslinked EMA, and the positive control cell suspension was washed, spun down and resuspended in culture medium. The scaffolds were then digested with collagenase (Worthington,  $600\ \mu\text{l}$  of  $0.6\ \text{mg}\ \text{ml}^{-1}$  collagenase in culture medium per scaffold in a 24-well plate) at  $37^{\circ}\text{C}$  for 15 min, followed by 15 min incubation on ice, with periodic pipetting to dissociate scaffolds and cell aggregates. The resulting cell suspension was added with 1 ml of medium, spun down and then resuspended in culture medium. The cell suspensions were subjected to FACS (Hospital for Sick Children Research Institute) to determine the percentage of EMA negative cells.

### 2.10. Statistical analysis

Statistical analysis was performed using SigmaStat 3.0 software. For comparison between two groups, Student's *t*-test was performed. For comparison between multiple groups, a one-way analysis of variance test was performed using the Holm–Sidak post-hoc test for pairwise compar-

isons; in the case of failed normality or unequal variance in the data set, Dunn's test was used for pairwise comparisons. Groups were considered significantly different with  $p < 0.05$ . All results are reported as mean  $\pm$  standard deviation.

## 3. Results and discussions

The Ultrafoam™ collagen sponge scaffold exhibited a macroporous structure consisting of interconnected pores

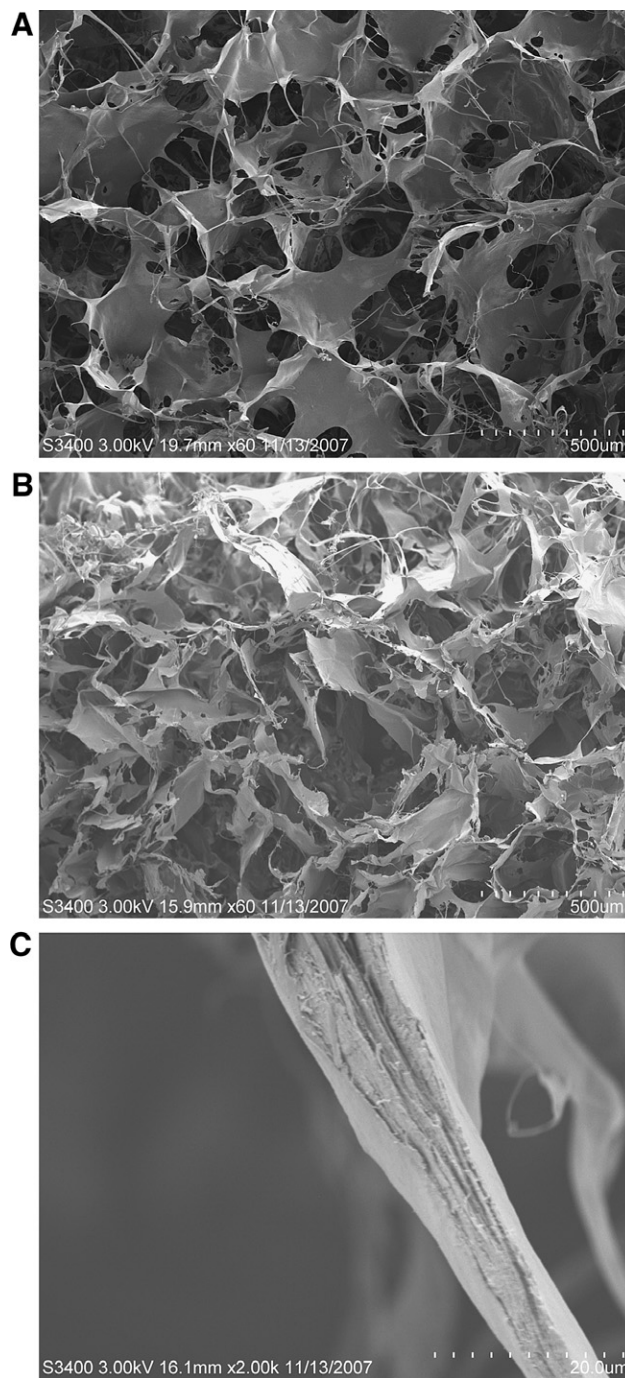


Fig. 1. Scanning electron microscopy of Ultrafoam™ collagen scaffold. (A) Face section; (B) cross-section; (C) cross-section of a pore wall.

of average diameter 190  $\mu\text{m}$  and an average wall thickness of 8  $\mu\text{m}$ . Pores as small as 1  $\mu\text{m}$  in diameter as well as fibers as small as 1.5  $\mu\text{m}$  in diameter were present within the structure of macropores (Fig. 1). We conjugated VEGF onto collagen scaffolds using EDC chemistry, which is a common method used to covalently couple proteins to biomaterials. For example, EDC was used to covalently couple rhBMP-2 onto silk fibroin films [27], to crosslink collagen with glycosaminoglycan [28] and to immobilize VEGF onto poly(acrylic acid) surfaces [22]. Here, we chose to use EDC chemistry to immobilize VEGF to the collagen scaffold because it is a stable, simple and water-based conjugation technique.

Immobilized VEGF was quantified in plane sections along the depth of the scaffold by a direct VEGF ELISA. Since the immobilization reaction was carried out by soaking the entire scaffold in reagent solutions, uniform immobilization was expected throughout the scaffold. Fig. 2a shows the concentrations of immobilized VEGF along the depth of the scaffold, in which there are no statistically significant differences among concentrations throughout the entire depth.

Importantly, VEGF was covalently immobilized to the scaffold and not simply adsorbed, as illustrated by the negligible amount of VEGF remaining in the scaffold when the EDC crosslinker was not used (Fig. 2a). Interestingly, the concentration of immobilized VEGF in the scaffolds was controlled by the concentration of EDC, as observed in Fig. 2b. Specifically, with a solution of VEGF at 500  $\text{ng ml}^{-1}$ , the concentration of immobilized VEGF in scaffold increased from  $38 \pm 5$  to  $56 \pm 10$   $\text{ng ml}^{-1}$  as the EDC crosslinker concentration increased from 4.8 to 24  $\text{mg ml}^{-1}$ . These concentrations correspond to a total of  $2.9 \pm 0.4$  and  $4.4 \pm 0.8$   $\text{ng scaffold}^{-1}$  of immobilized VEGF, respectively. (The data in Fig. 2 are expressed in terms of concentration assuming that the scaffold is a cylinder of 7 mm diameter and 2 mm thickness.) As will become apparent, this concentration of immobilized VEGF was suitable for our purposes of promoting cell penetration into the scaffolds; however, we note that the crosslinking efficiency can be further improved by using a buffer at a lower pH.

Having established that VEGF was immobilized on the collagen scaffolds, we investigated the effect of immobilized

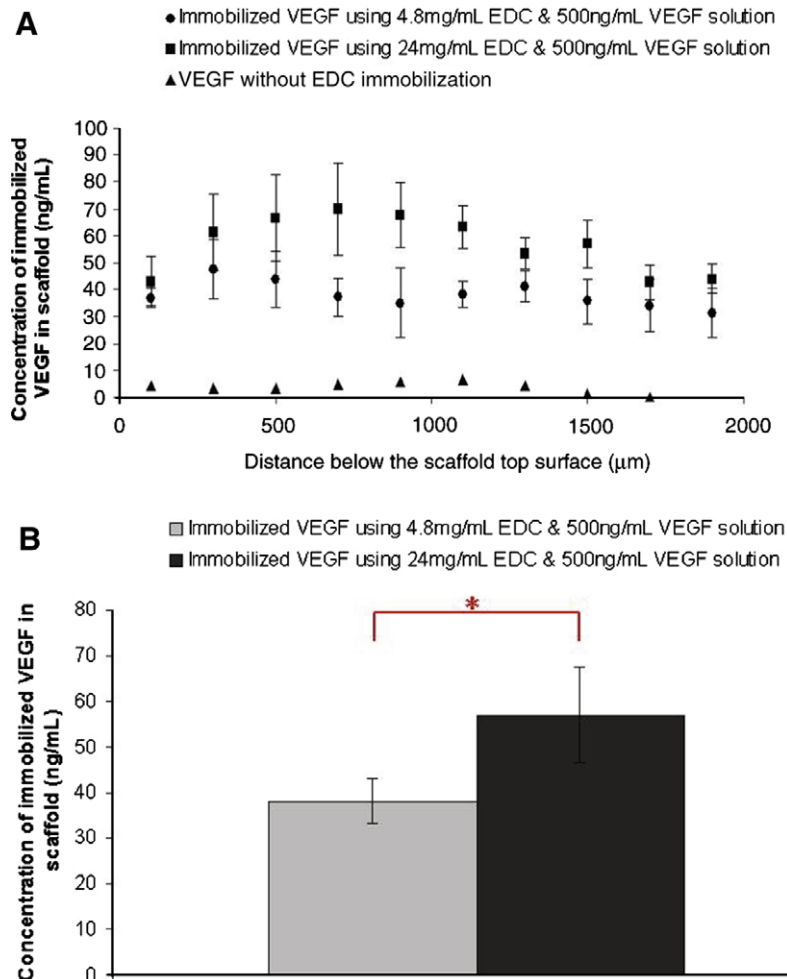


Fig. 2. Concentration of immobilized VEGF in the porous 3D collagen scaffold. (A) Concentration of immobilized VEGF along the depth of the scaffold ( $n = 3$ , no statistically significant differences among concentrations along the depth of the scaffold). (B) Average concentration of immobilized VEGF within the scaffold. \* Statistically significant difference,  $p < 0.05$ .

VEGF on the growth of ECs in the collagen scaffolds. Immediately after seeding, the cell density was low and uniform in the entire cross-section of the scaffold (Fig. 3). We compared cell growth over 1 week in the following scaffolds: scaffolds with approximately  $40 \text{ ng ml}^{-1}$  immobilized VEGF (using  $4.8 \text{ mg ml}^{-1}$  EDC and  $500 \text{ ng ml}^{-1}$  VEGF

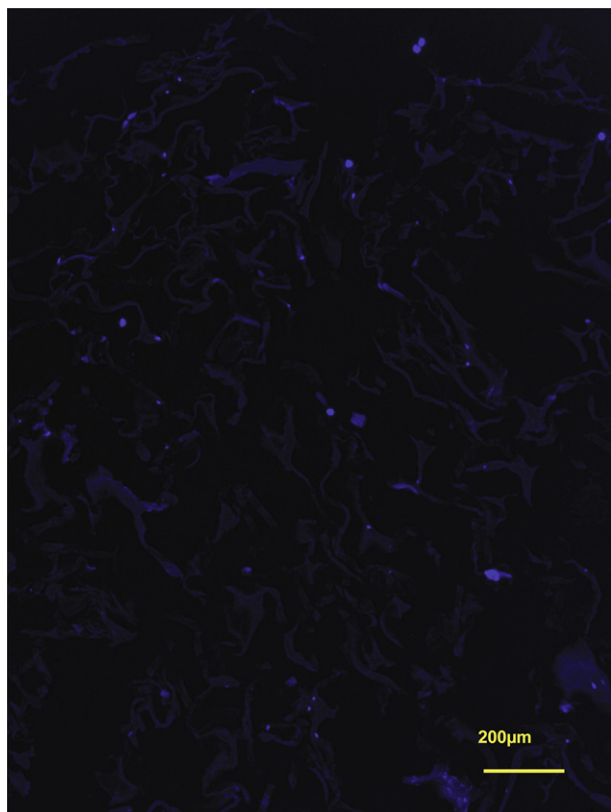


Fig. 3. Cross-section of the collagen scaffold immediately after seeding of D4T cells. The cell nuclei were stained with DAPI (appearing dark blue). Collagen scaffold appears light blue. (For interpretation of the references in color in this figure legend, the reader is referred to the web version of this article.)

solution, as shown in Fig. 2b, total amount of VEGF  $2.9 \text{ ng scaffold}^{-1}$ ), scaffolds with approximately  $110 \text{ ng ml}^{-1}$  immobilized VEGF (using  $24 \text{ mg ml}^{-1}$  EDC and  $1 \mu\text{g ml}^{-1}$  VEGF solution total amount of VEGF  $8.8 \text{ ng scaffold}^{-1}$ ; immobilized concentration and total amount were estimated based on Fig. 2b, since it was above the detection limit of the direct VEGF ELISA method), scaffolds cultured in culture medium containing  $100 \text{ ng ml}^{-1}$  soluble VEGF and control scaffolds without VEGF. We consistently observed statistically higher cell density at every depth within those scaffolds with immobilized VEGF compared with the control scaffolds without VEGF and those scaffolds cultured with soluble VEGF in the culture medium (Fig. 4). This suggests that immobilized VEGF promotes greater EC penetration into the collagen scaffold. As shown in Fig. 5, the cell density in the scaffolds with immobilized VEGF was uniformly high throughout the scaffold, whereas the cell density in control and soluble VEGF scaffolds was rather sparse. Fig. 6 shows the immunohistochemistry of the CD31 marker on ECs cultured in different scaffolds, where the higher cell density is apparent along the depth of the scaffolds with immobilized VEGF compared with both control scaffolds, having either no VEGF or soluble VEGF in the culture medium.

We estimated the number of ECs after 1 week of culture in the same group of scaffolds using the XTT assay. To convert the XTT absorbance measurements to the number of cells residing in scaffolds after 1 week, we seeded a series of scaffolds with known numbers of cells and used these to create a standard curve. As shown in Fig. 7, after 1 week of culture, more cells were present within scaffolds with immobilized VEGF compared with the scaffolds without VEGF and scaffolds cultured in soluble VEGF. After 1 week, the number of cells in scaffolds with immobilized VEGF was about seven times that of the cell number seeded originally, while the numbers of cells in scaffolds without VEGF and in scaffolds cultured in soluble VEGF were less than double the cell number seeded originally. This finding

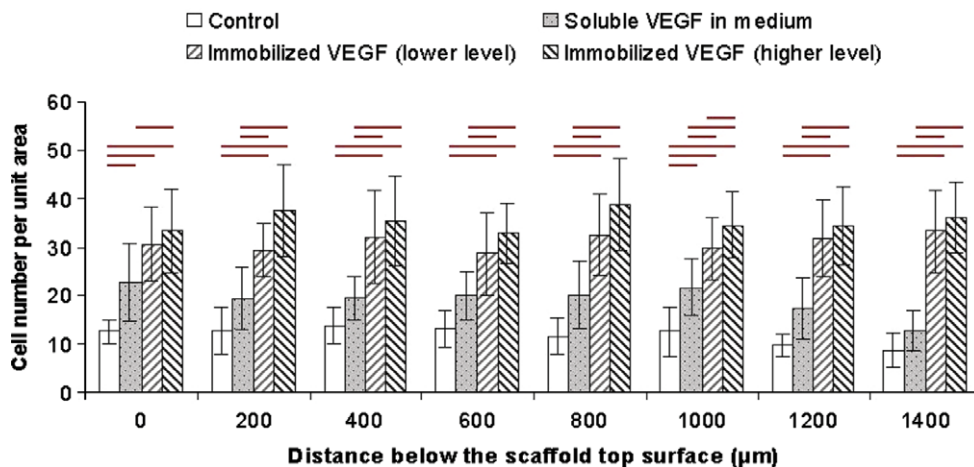


Fig. 4. EC density along the depth of the scaffold after 1 week of culture. Scaffolds were cultivated without VEGF (control), in culture medium containing  $100 \text{ ng ml}^{-1}$  soluble VEGF, on scaffolds with immobilized VEGF (lower level,  $\sim 40 \text{ ng ml}^{-1}$ ) or on scaffolds with immobilized VEGF (higher level,  $\sim 110 \text{ ng ml}^{-1}$ ).  $n = 3$ ; lines above data columns denote statistically significant differences,  $p < 0.05$ .

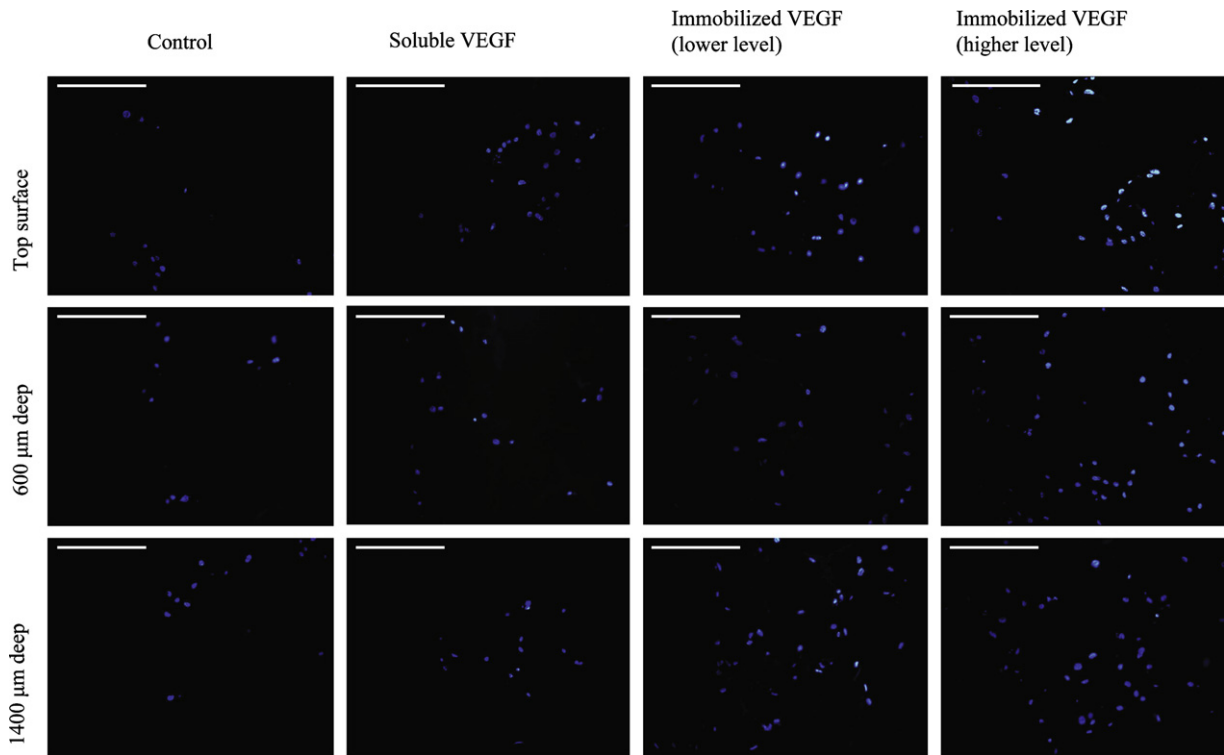


Fig. 5. Representative DAPI nuclear stain images showing the cell density along depth of the scaffold after 1 week of culture, as quantified in Fig. 2. Scaffolds were cultivated without VEGF (control), in culture medium containing  $100 \text{ ng ml}^{-1}$  soluble VEGF, on scaffolds with immobilized VEGF (lower level,  $\sim 40 \text{ ng ml}^{-1}$ ) or on scaffolds with immobilized VEGF (higher level,  $\sim 110 \text{ ng ml}^{-1}$ ). Scale bar:  $200 \mu\text{m}$ .

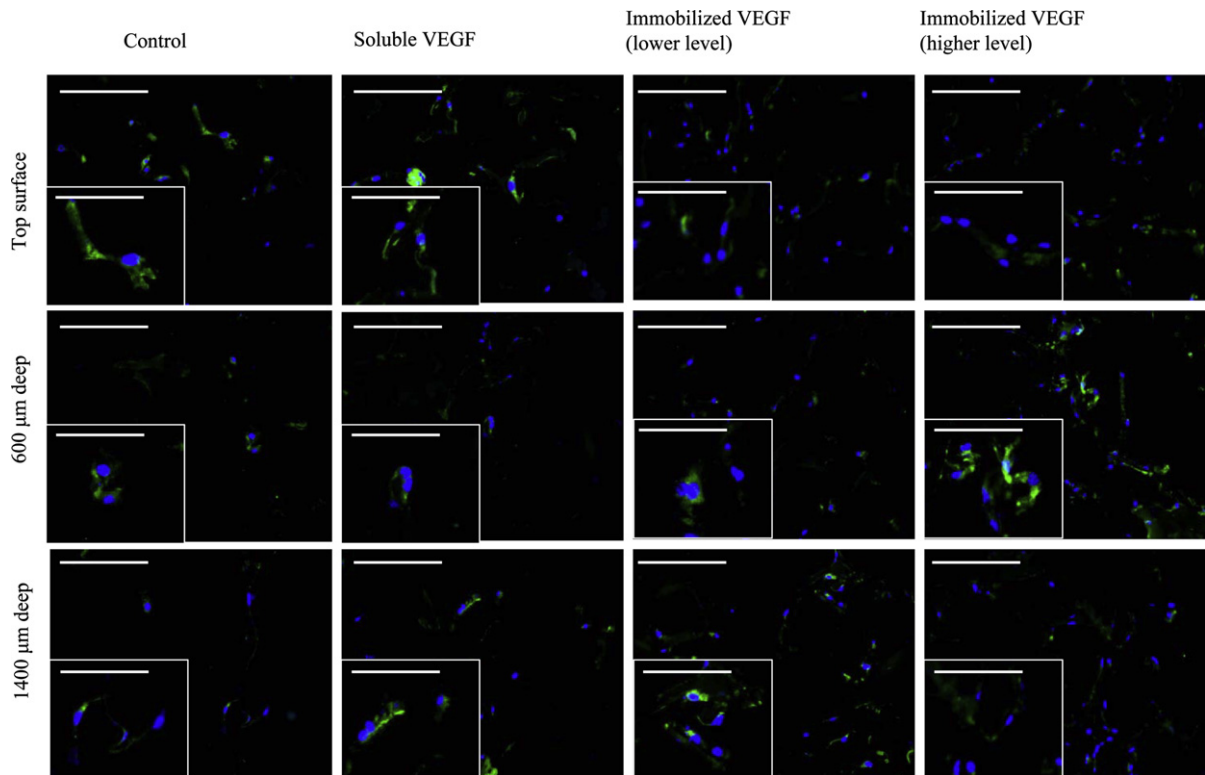


Fig. 6. Representative CD31 immunohistochemistry images showing EC distribution along depth of the scaffold after 1 week of culture. Scaffolds were cultivated without VEGF (control), in culture medium containing  $100 \text{ ng ml}^{-1}$  soluble VEGF, on scaffolds with immobilized VEGF (lower level,  $\sim 40 \text{ ng ml}^{-1}$ ) or on scaffolds with immobilized VEGF (higher level,  $\sim 110 \text{ ng ml}^{-1}$ ). Blue: DAPI nuclear stain; green: CD31; scale bar:  $200 \mu\text{m}$ . Inset scale bar:  $100 \mu\text{m}$ . (For interpretation of the references in color in this figure legend, the reader is referred to the web version of this article.)

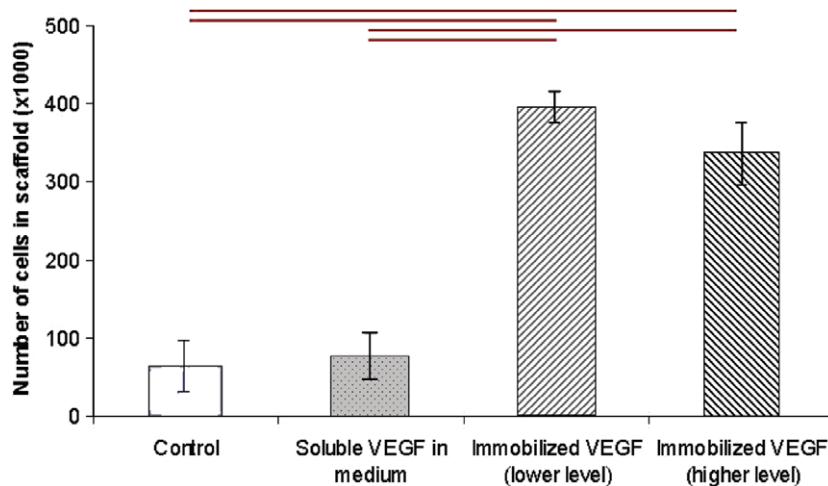


Fig. 7. Estimated number of cells residing within the scaffold after 1 week of culture, measured by XTT proliferation assay. Scaffolds were cultivated without VEGF (control), in culture medium containing  $100 \text{ ng ml}^{-1}$  soluble VEGF, on scaffolds with immobilized VEGF (lower level,  $\sim 40 \text{ ng ml}^{-1}$ ) or on scaffolds with immobilized VEGF (higher level,  $\sim 110 \text{ ng ml}^{-1}$ ).  $n = 3$ ; lines above data columns denote statistically significant differences,  $p < 0.05$ .

indicates that immobilized VEGF promotes greater proliferation of ECs in collagen scaffolds, which is consistent with results from the cell density analysis (Fig. 4).

We measured the level of glucose and lactate in the culture medium during the 1 week culture of ECs in the same group of scaffolds, because glucose consumption and lactate production are indicators of the net metabolic activity of the cells. As shown in Figs. 8 and 9, the rate of glucose consumption and the rate of lactate production were significantly higher for ECs cultured in scaffolds with immobilized VEGF compared to scaffolds without VEGF and scaffolds cultured in soluble VEGF over time. The increased metabolic activities by the glucose or the lactate assays are due to the increased cell number in scaffolds with immobilized VEGF. As such, the glucose and lactate assays serve as an additional independent measure of the cell num-

ber. For example, at day 7 the lactate production rate was on the order of  $1 \times 10^{-5} \mu\text{mol cell}^{-1} \text{ day}^{-1}$  for all groups ( $1.3, 1.2, 0.7$  and  $0.8 \times 10^{-5} \mu\text{mol cell}^{-1} \text{ day}^{-1}$  for the control, soluble VEGF, immobilized VEGF (lower level) and immobilized VEGF (higher level), respectively). The average glucose consumption rate per cell at the end of cultivation was  $1.6, 1.5, 0.6$  and  $0.7 \times 10^{-5} \mu\text{mol cell}^{-1} \text{ day}^{-1}$  for the control, soluble VEGF, immobilized VEGF (lower level) and immobilized VEGF (higher level), respectively.

Throughout the cultivation period, the molar ratio of lactate produced to glucose consumed (L/G) was  $\leq 1$  for scaffolds without VEGF and scaffolds cultured in soluble VEGF, indicating aerobic cell metabolism, which is consistent with the lower cell density in these groups. At a low cell density, diffusional transport alone is capable of meeting the oxygen demand of the 3D tissue. In contrast, for

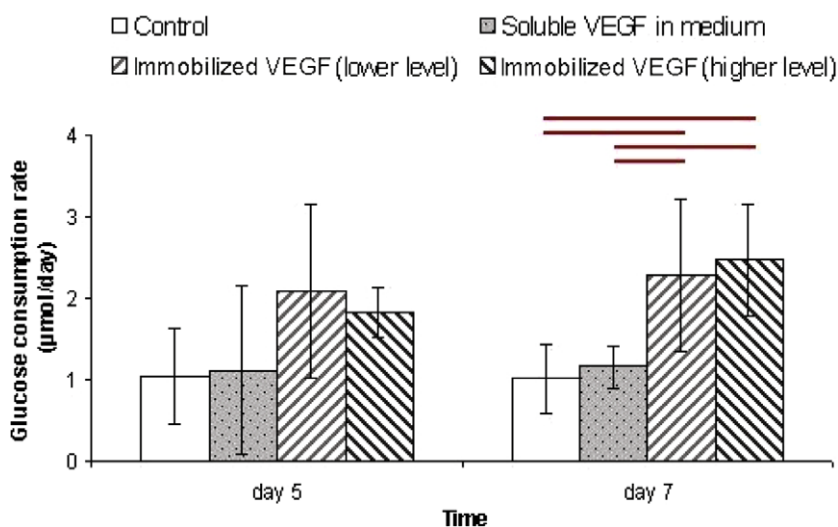


Fig. 8. Glucose consumption rate of ECs in scaffolds during 1 week culture. Scaffolds were cultivated without VEGF (control), in culture medium containing  $100 \text{ ng ml}^{-1}$  soluble VEGF, on scaffolds with immobilized VEGF (lower level,  $\sim 40 \text{ ng ml}^{-1}$ ) or on scaffolds with immobilized VEGF (higher level,  $\sim 110 \text{ ng ml}^{-1}$ ).  $n = 3$ ; lines above data columns denote statistically significant differences,  $p < 0.05$ .

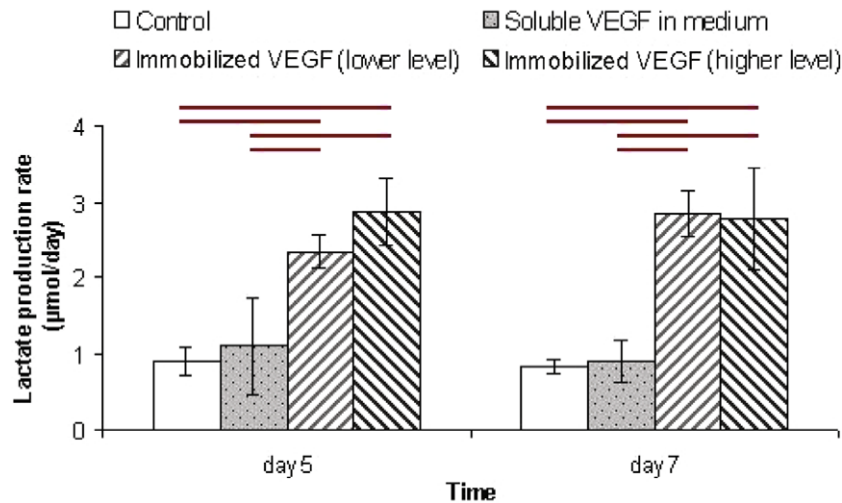


Fig. 9. Lactate production rate of ECs in scaffolds during 1 week culture. Scaffolds were cultivated without VEGF (control), in culture medium containing  $100 \text{ ng ml}^{-1}$  soluble VEGF, on scaffolds with immobilized VEGF (lower level,  $\sim 40 \text{ ng ml}^{-1}$ ) or on scaffolds with immobilized VEGF (higher level,  $\sim 110 \text{ ng ml}^{-1}$ ).  $n = 3$ ; lines above data columns denote statistically significant differences,  $p < 0.05$ .

cells cultured in scaffolds with immobilized VEGF, the L/G was in the range of 1.2–1.6. This indicates the onset of anaerobic cell metabolism, which is associated with the limitations of oxygen diffusion in high cell density 3D tissues cultivated under static condition [5].

VEGF-immobilized in the collagen scaffold, elicited a significantly greater effect on ECs compared with  $100 \text{ ng ml}^{-1}$  soluble VEGF added into the culture medium, even though the concentration of immobilized VEGF ( $\sim 40 \text{ ng ml}^{-1}$ ) in the scaffold was lower compared with the concentration of soluble VEGF in the culture medium. When comparing the total amount of VEGF present, there was a total of 60 ng of soluble VEGF present in the culture medium (scaffold cultured in  $600 \mu\text{l}$  of culture medium containing  $100 \text{ ng ml}^{-1}$  soluble VEGF) compared with much lesser amounts of 2.9 ng (lower level) and 8.8 ng (higher level) of immobilized VEGF in the scaffold. Furthermore, the culture medium was exchanged twice during the 1 week culture, thus an even greater amount of VEGF was presented to scaffolds cultured with soluble VEGF.

The greater effect of immobilized VEGF compared with soluble VEGF observed here is likely due to the immobilized growth factors providing a controlled and sustainable influence on cell behavior vs. the transient effect of soluble growth factors [24,29]. Immobilized growth factors promote a local regulation and guidance of cellular activity, which can mimic the microenvironment in vivo [8,30,31]. In our case, the immobilized VEGF in collagen scaffold likely provided a cue to guide the infiltration and proliferation of ECs in the porous matrix. In addition, immobilized growth factors can provide extended signaling since the ligand will not be internalized as a ligand/receptor complex [22,24]. It is known that binding of growth factors to cell surface receptors often leads to internalization of the receptor/ligand complex followed by degradation of the receptor. Interestingly, VEGF induces receptor/ligand

internalization in ECs, and it has been reported that up to 70% of the receptor/ligand complexes were internalized in ECs following 1 h of incubation with VEGF [11]. Receptor internalization is one of the self-regulating mechanisms by which cells become desensitized to continuous growth factor activation. It is still unclear whether some functions of VEGF signal transduction might require internalization [11,32], but various studies along with ours indicate that immobilized VEGF is capable of activating signal transduction pathways to achieve the desired EC responses [22–25]. The immobilized VEGF is capable of continuously stimulating EC growth by inhibiting the down-regulation of receptor/ligand complex internalization, therefore demonstrating greater effect than soluble VEGF. Interestingly, Taguchi and colleagues also reported that a lower concentration of VEGF on polymer films with co-immobilized fibronectin and VEGF resulted in greater proliferative effect on ECs compared with a higher concentration of soluble VEGF [22], which is in agreement with our findings. We did not observe a substantial difference in the effect elicited by the higher ( $\sim 110 \text{ ng ml}^{-1}$ ) vs. the lower ( $\sim 40 \text{ ng ml}^{-1}$ ) level of immobilized VEGF, possibly because the VEGF signaling saturation has been reached.

Results from the XTT proliferation assay (Fig. 7) and glucose/lactate metabolism assays (Figs. 8 and 9) show that  $100 \text{ ng ml}^{-1}$  soluble VEGF added to the culture medium did not induce a significant increase in the proliferation of ECs in collagen scaffolds compared with control scaffolds without VEGF. A likely explanation is that soluble VEGF in the bulk medium may not be able to reach the interior of the porous 3D scaffold, due to either diffusional limitations or being actively taken up by cells residing on the peripheral surfaces of the scaffold. It is possible that dynamic culture conditions, under orbital shaking or perfusion, would increase the availability of the soluble VEGF to the interior of the cell-seeded scaffold. Soluble VEGF added to the cul-

ture medium can stimulate the growth of ECs plated on two-dimensional substrates [22,24,25], so VEGF immobilization is not required in 2D. However, the addition of growth factors to bulk medium has not been typically used to induce cell growth in 3D matrices. Most studies that aim to promote vascularization within a 3D scaffold use strategies to maintain a sustained delivery of angiogenic growth factors within the scaffold, such as the encapsulation of growth factors in scaffolds or microspheres for controlled release [8,13–16]. Such strategies maintain a steady supply of growth factors in the scaffold, which is required to induce angiogenesis within the engineered tissue constructs.

We investigated the viability of ECs after 1 week of culture in the same group of scaffolds. As shown in Fig. 10, we observed significantly higher viability of ECs cultured in scaffolds with immobilized VEGF in comparison with both scaffolds without VEGF and scaffolds cultured in soluble VEGF. The viability of ECs cultured in scaffolds with immobilized VEGF is comparable with that of ECs grown in the T75 culture flask (used as a positive control). This result suggests that immobilized VEGF promotes the survival of ECs in collagen scaffolds. While we did not probe the mechanism, there are several reports that suggest possible mechanisms of VEGF regulating EC survival. For example, Nor and colleagues found that VEGF enhanced EC survival by inducing the expression of Bcl-2, an anti-apoptotic protein [33]. Gerber and colleagues found that VEGF regulated EC survival through flk-1/KDR activation, leading to the PI3-kinase/Akt signal transduction pathway [34]. Interestingly, Hutchings and colleagues found that ECs can adhere and migrate on immobilized isoforms of VEGF, mediated by several integrin receptors [35]. Furthermore, they demonstrated that immobilized VEGF-promoted the migration and survival of ECs through interactions with integrins. These findings potentially explain our observation of increased EC viability in collagen scaffolds with immobilized VEGF.

Since proteases present in the serum of the culture medium contribute to the enzymatic degradation of collagen scaffold, we performed a scaffold degradation study in the culture medium, with periodic medium exchange, to reproduce the conditions a scaffold experiences during cell culture. The scaffold dry weights were  $4.0 \pm 0.3$ ,  $3.6 \pm 0.5$  and  $2.4 \pm 0.5$  mg after 10 min, 7 days and 12 days in the culture medium, respectively. In this rigorous model, there was no significant difference in the scaffold dry weight after 10 min and 7 days ( $p = 0.556$ ), indicating that negligible degradation of collagen scaffold occurred in this time period. The time period of 7 days corresponds to the duration of cell culture in the current study. Thus, most of the proliferative and survival effects of VEGF observed in the current study may be attributed to the immobilized VEGF. In contrast, there was a significant decrease in the dry weight of the scaffolds maintained in the culture medium for 12 days ( $p = 0.012$  for 10 min vs. 12 days;  $p = 0.04$  for 7 days vs. 12 days), indicating that at longer time points some immobilized VEGF may be released into the culture medium as a result of scaffold degradation. The collagen scaffold was observed to slightly decrease in its length and width during culture, which is consistent with the well-known phenomenon of cell traction that leads to scaffold compaction [36]. For cell-free scaffolds maintained in the culture medium up to 12 days, the decrease in size was not observed (data not shown).

VEGF receptor 2 (VEGFR2 also known as Flk1 or KDR) is considered to be the major mediator of physiological effects such as proliferation, migration, survival and tube formation caused by VEGF<sub>165</sub> [37], a growth factor used in the current study. Binding of the VEGF to VEGFR2 causes receptor dimerization and autophosphorylation, followed by the activation of a number of downstream pathways of which activation of extracellular regulated kinase (Erk) pathway regulates proliferation [37]. In this work, we presented evidence based on

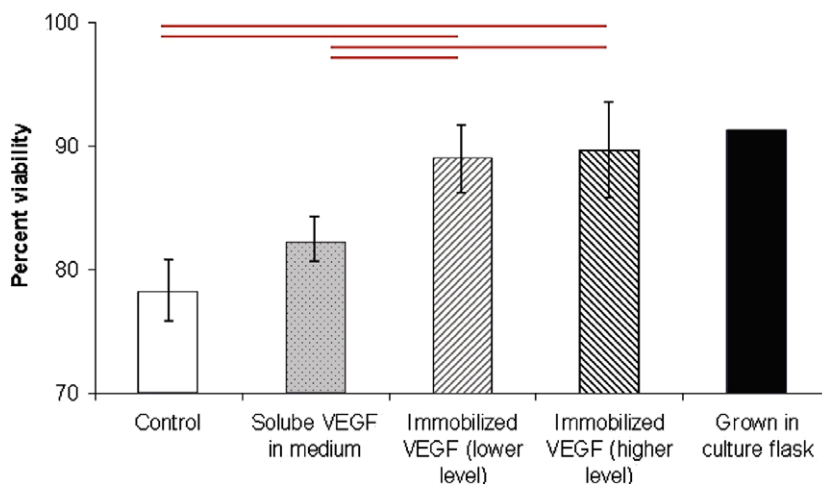


Fig. 10. Viability of ECs in scaffolds after 1 week culture. Scaffolds were cultivated without VEGF (control), in culture medium containing  $100 \text{ ng ml}^{-1}$  soluble VEGF, on scaffolds with immobilized VEGF (lower level,  $\sim 40 \text{ ng ml}^{-1}$ ) or on scaffolds with immobilized VEGF (higher level,  $\sim 110 \text{ ng ml}^{-1}$ ).  $n = 3$ ; lines above data columns denote statistically significant differences,  $p < 0.05$ .

histological (Fig. 4) and metabolic (XTT, glucose, lactate, Figs. 7–9) assays that immobilized VEGF-promoted proliferation of endothelial cells in 3D collagen scaffolds. We also demonstrated that cell viability was higher on the VEGF-immobilized scaffolds compared with the controls, consistent with the ability of VEGF to promote survival through the Akt/PKB pathway [37]. The significantly higher density of endothelial cells deep ( $\geq 1000 \mu\text{m}$ ) within the scaffolds with immobilized VEGF may be due to either proliferation or migration (Fig. 4). However, we have not conclusively observed tube formation in the current system (Fig. 6). Further studies modulating VEGF concentration, cell seeding density and duration of culture are required to yield tube formation in this system.

Since EDC conjugation results in the formation of a direct amide link between VEGF and the collagen scaffold, we were concerned that the immobilized VEGF may lose bioactivity. However, the *in vitro* cell studies presented above confirmed that the immobilized VEGF remained bioactive in the collagen scaffold. Taguchi and colleagues also demonstrated that VEGF-immobilized onto polymer films using EDC chemistry maintained bioactivity, which agrees with our findings [22]. In our approach, the carboxylic groups on the collagen scaffold were activated by immersing the scaffold in EDC/NHS solution for 20 min. Upon addition of VEGF<sub>165</sub>, the activated carboxylic groups are expected to react with amine groups on the VEGF molecule. VEGF<sub>165</sub> is a homodimer of two molecules covalently linked via cysteine residues (Cys-51 of one molecule with Cys-60 of the other molecule) [38–40]. Each homodimer contains two binding sites for VEGFR2. The amino acid sequences from both molecules in the homodimer make up the binding cleft. There are 66 amine groups on the outer surface of the VEGF<sub>165</sub> homodimer, four of which are located in the VEGFR2 binding clefts [38–40], thus the probability that the binding pocket was affected during grafting of VEGF to collagen scaffold is estimated to be 6.06%. Upon activation, the scaffold is removed from the EDC/NHS solution and the VEGF solution is applied immediately (without a rinsing step in between). Thus, there is a small possibility that the remaining EDC/NHS caused crosslinking of some VEGF molecules themselves and also some collagen molecules themselves.

The immobilization of VEGF onto 3D scaffolds has not been widely explored in tissue engineering applications. Several groups have conjugated VEGF onto 2D substrates with the motivation of inducing endothelialization of the biomaterial [22–25]. These studies showed increased proliferation of ECs on VEGF-immobilized substrates. Koch and colleagues immobilized VEGF in 3D collagen matrices using a homobifunctional crosslinker, with the goal of enhancing angiogenesis in wound healing applications [41]. They demonstrated that ECs cultured in a 2D tissue culture plate showed increased proliferation upon exposure to VEGF-immobilized collagen matrices *in vitro*; furthermore, VEGF-immobilized collagen matrices enhanced

angiogenesis of the surrounding environment upon implantation into the chorioallantoic membrane of the chicken embryo.

Here, we were interested in using scaffolds with immobilized growth factors to control cell behavior in tissue engineering applications. We demonstrated that VEGF-immobilized in porous 3D collagen scaffolds promoted EC proliferation and infiltration more efficiently than soluble VEGF added to the culture medium. Thus, immobilization of VEGF may be a useful approach to control EC proliferation in tissue engineering.

The most studied approach to inducing vascularization in engineered tissues is the sustained delivery of angiogenic growth factors to promote vessel sprouting from surrounding tissue into the engineered tissue post-implantation [8,13–16]. In another approach, both ECs and tissue-specific cells are co-cultured in the scaffold, with the aim of forming prevascularized networks to support tissue assembly and survival [1,42–44]. In order to achieve prevascularization of the engineered tissue *in vitro*, a high density of ECs needs to be uniformly distributed within the 3D matrix, which would subsequently assemble into vascular networks [7].

Our work indicates that immobilization of angiogenic growth factors within a 3D scaffold may be a promising strategy to induce the assembly of a high density of ECs in the scaffold and to guide its vascularization process in a controlled manner. By immobilizing VEGF in a 3D porous collagen scaffold using EDC chemistry, we showed that immobilized VEGF promotes the infiltration and proliferation of ECs in the collagen scaffold for ultimate application in tissue engineering. We demonstrated that immobilized VEGF could enhance the assembly of a high density of ECs in the collagen scaffold, which is a first step in achieving vascularization within the engineered tissue constructs. Future work will aim to optimize the conditions to drive the vascularization of ECs in scaffolds with immobilized VEGF, and also attempt to co-culture tissue-specific cells in EC prevascularized scaffolds with immobilized VEGF.

#### 4. Conclusion

We conjugated VEGF onto a porous 3D collagen scaffold using EDC chemistry, with the aim of promoting the penetration and assembly of a high density of ECs into the scaffold. The immobilized VEGF in collagen scaffolds was bioactive and promoted the penetration and proliferation of ECs in the collagen scaffold according to cell density analysis in histological sections, immunohistochemistry, XTT proliferation assay, glucose consumption and lactate production. Importantly, EC viability was greater on scaffolds with immobilized VEGF than controls. As a first step to inducing vascularization within engineered tissue constructs, our work demonstrates that immobilization of VEGF is a useful strategy to promote the invasion and assembly of a high density of ECs in the collagen scaffold.

## Acknowledgements

This study was supported by an NSERC Discovery Grant (M.R.) and an LOF Grant from Canada Foundation for Innovation (M.R.). The authors thank Ms. Lorraine Chiu for help with the scaffold degradation study.

## References

- [1] Caspi O, Lesman A, Basevitch Y, Gepstein A, Arbel G, Habib IH, et al. Tissue engineering of vascularized cardiac muscle from human embryonic stem cells. *Circ Res* 2007;100:263–72.
- [2] Morritt AN, Bortolotto SK, Dilley RJ, Han X, Kompa AR, McCombe D, et al. Cardiac tissue engineering in an in vivo vascularized chamber. *Circulation* 2007;115:353–60.
- [3] Radisic M, Euloth M, Yang L, Langer R, Freed LE, Vunjak-Novakovic G. High-density seeding of myocyte cells for cardiac tissue engineering. *Biotechnol Bioeng* 2003;82:403–14.
- [4] Radisic M, Yang L, Boublik J, Cohen RJ, Langer R, Freed LE, et al. Medium perfusion enables engineering of compact and contractile cardiac tissue. *Am J Physiol Heart Circ Physiol* 2004;286:H507–16.
- [5] Radisic M, Malda J, Epping E, Geng W, Langer R, Vunjak-Novakovic G. Oxygen gradients correlate with cell density and cell viability in engineered cardiac tissue. *Biotechnol Bioeng* 2006;93:332–43.
- [6] Freed LE, Guilak F, Guo XE, Gray ML, Tranquillo R, Holmes JW, et al. Advanced tools for tissue engineering: scaffolds, bioreactors, and signaling. *Tissue Eng* 2006;12:3285–305.
- [7] Laschke MW, Harder Y, Amon M, Martin I, Farhadi J, Ring A, et al. Angiogenesis in tissue engineering: breathing life into constructed tissue substitutes. *Tissue Eng* 2006;12:2093–104.
- [8] Boonthekul T, Mooney DJ. Protein-based signaling systems in tissue engineering. *Curr Opin Biotechnol* 2003;14:559–65.
- [9] Ahrendt G, Chickering DE, Ranieri JP. Angiogenic growth factors: a review for tissue engineering. *Tissue Eng* 1998;4.
- [10] Neufeld G, Cohen T, Gengrinovitch S, Poltorak Z. Vascular endothelial growth factor (VEGF) and its receptors. *FASEB J* 1999;13:9–22.
- [11] Dougher M, Terman BI. Autophosphorylation of KDR in the kinase domain is required for maximal VEGF-stimulated kinase activity and receptor internalization. *Oncogene* 1999;18:1619–27.
- [12] Olsson AK, Dimberg A, Kreuger J, Claesson-Welsh L. VEGF receptor signalling – in control of vascular function. *Nat Rev Mol Cell Biol* 2006;7:359–71.
- [13] Richardson TP, Peters MC, Ennett AB, Mooney DJ. Polymeric system for dual growth factor delivery. *Nat Biotechnol* 2001;19:1029–34.
- [14] Smith MK, Peters MC, Richardson TP, Garbern JC, Mooney DJ. Locally enhanced angiogenesis promotes transplanted cell survival. *Tissue Eng* 2004;10:63–71.
- [15] Murphy WL, Peters MC, Kohn DH, Mooney DJ. Sustained release of vascular endothelial growth factor from mineralized poly(lactide-co-glycolide) scaffolds for tissue engineering. *Biomaterials* 2000;21:2521–7.
- [16] Perets A, Baruch Y, Weisbuch F, Shoshany G, Neufeld G, Cohen S. Enhancing the vascularization of three-dimensional porous alginate scaffolds by incorporating controlled release basic fibroblast growth factor microspheres. *J Biomed Mater Res A* 2003;65:489–97.
- [17] Ferreira LS, Gerecht S, Fuller J, Shieh HF, Vunjak-Novakovic G, Langer R. Bioactive hydrogel scaffolds for controllable vascular differentiation of human embryonic stem cells. *Biomaterials* 2007;28:2706–17.
- [18] Yeo Y, Geng W, Ito T, Kohane DS, Burdick JA, Radisic M. Photocrosslinkable hydrogel for myocyte cell culture and injection. *J Biomed Mater Res B Appl Biomater* 2006;81B:312–22.
- [19] Sigrist S, Mechine-Neuville A, Mandes K, Calenda V, Braun S, Legeay G, et al. Influence of VEGF on the viability of encapsulated pancreatic rat islets after transplantation in diabetic mice. *Cell Transplant* 2003;12:627–35.
- [20] Ito Y, Liu SQ, Imanishi Y. Enhancement of cell growth on growth factor-immobilized polymer film. *Biomaterials* 1991;12:449–53.
- [21] Ito Y, Zheng J, Imanishi Y, Yonezawa K, Kasuga M. Protein-free cell culture on an artificial substrate with covalently immobilized insulin. *Proc Natl Acad Sci USA* 1996;93:3598–601.
- [22] Taguchi T, Kishida A, Akashi M, Maruyama I. Immobilization of human vascular endothelial growth factor (VEGF165) onto biomaterials: an evaluation of the biological activity of immobilized VEGF165. *J Bioact Comp Polym* 2000;15:309–20.
- [23] Ito Y, Hasuda H, Terai H, Kitajima T. Culture of human umbilical vein endothelial cells on immobilized vascular endothelial growth factor. *J Biomed Mater Res A* 2005;74:659–65.
- [24] Backer MV, Patel V, Jehning BT, Claffey KP, Backer JM. Surface immobilization of active vascular endothelial growth factor via a cysteine-containing tag. *Biomaterials* 2006;27:5452–8.
- [25] Zisch AH, Schenk U, Schense JC, Sakiyama-Elbert SE, Hubbell JA. Covalently conjugated VEGF–fibrin matrices for endothelialization. *J Control Release* 2001;72:101–13.
- [26] Kennedy M, Keller GM. Hematopoietic commitment of ES cells in culture. *Methods Enzymol* 2003;365:39–59.
- [27] Karageorgiou V, Meinel L, Hofmann S, Malhotra A, Volloch V, Kaplan D. Bone morphogenetic protein-2 decorated silk fibroin films induce osteogenic differentiation of human bone marrow stromal cells. *J Biomed Mater Res A* 2004;71:528–37.
- [28] Pieper JS, Hafmans T, van Wachem PB, van Luyn MJ, Brouwer LA, Veerkamp JH, van Kuppevelt TH. Loading of collagen–heparan sulfate matrices with bFGF promotes angiogenesis and tissue generation in rats. *J Biomed Mater Res* 2002;62:185–94.
- [29] Vasita R, Katti DS. Growth factor-delivery systems for tissue engineering: a materials perspective. *Expert Rev Med Dev* 2006;3:29–47.
- [30] Kapur TA, Shoichet MS. Immobilized concentration gradients of nerve growth factor guide neurite outgrowth. *J Biomed Mater Res A* 2004;68:235–43.
- [31] Moore K, MacSween M, Shoichet M. Immobilized concentration gradients of neurotrophic factors guide neurite outgrowth of primary neurons in macroporous scaffolds. *Tissue Eng* 2006;12:267–78.
- [32] Li W, Keller G. VEGF nuclear accumulation correlates with phenotypical changes in endothelial cells. *J Cell Sci* 2000;113:1525–34.
- [33] Nor JE, Christensen J, Mooney DJ, Polverini PJ. Vascular endothelial growth factor (VEGF)-mediated angiogenesis is associated with enhanced endothelial cell survival and induction of Bcl-2 expression. *Am J Pathol* 1999;154:375–84.
- [34] Gerber HP, McMurtrey A, Kowalski J, Yan M, Keyt BA, Dixit V, et al. Vascular endothelial growth factor regulates endothelial cell survival through the phosphatidylinositol 3′-kinase/Akt signal transduction pathway. Requirement for Flk-1/KDR activation. *J Biol Chem* 1998;273:30336–43.
- [35] Hutchings H, Ortega N, Plouet J. Extracellular matrix-bound vascular endothelial growth factor promotes endothelial cell adhesion, migration, and survival through integrin ligation. *FASEB J* 2003;17:1520–2.
- [36] Enever PA, Shreiber DI, Tranquillo RT. A novel implantable collagen gel assay for fibroblast traction and proliferation during wound healing. *J Surg Res* 2002;105:160.
- [37] Cross MJ, Dixelius J, Matsumoto T, Claesson-Welsh L. VEGF-receptor signal transduction. *Trends Biochem Sci* 2003;28:488.
- [38] Muller YA, Li B, Christinger HW, Wells JA, Cunningham BC, de Vos AM. Vascular endothelial growth factor: crystal structure and functional mapping of the kinase domain receptor binding site. *Proc Natl Acad Sci USA* 1997;94:7192.
- [39] Walsh TP, Grant GH. Computer modelling of the receptor-binding domains of VEGF and PlGF. *Protein Eng* 1997;10:389.

- [40] Krilleke D, DeErkenez A, Schubert W, Giri I, Robinson GS, Ng YS, et al. Molecular mapping and functional characterization of the VEGF164 heparin-binding domain. *J Biol Chem* 2007;282:28045.
- [41] Koch S, Yao C, Grieb G, Prevel P, Noah EM, Steffens GC. Enhancing angiogenesis in collagen matrices by covalent incorporation of VEGF. *J Mater Sci Mater Med* 2006;17:735–41.
- [42] Narmoneva DA, Vukmirovic R, Davis ME, Kamm RD, Lee RT. Endothelial cells promote cardiac myocyte survival and spatial reorganization: implications for cardiac regeneration. *Circulation* 2004;110:962–8.
- [43] Kaihara S, Borenstein J, Koka R, Lalan S, Ochoa ER, Ravens M, et al. Silicon micromachining to tissue engineer branched vascular channels for liver fabrication. *Tissue Eng* 2000;6:105–17.
- [44] Helm CL, Zisch A, Swartz MA. Engineered blood and lymphatic capillaries in 3D VEGF–fibrin–collagen matrices with interstitial flow. *Biotechnol Bioeng* 2007;96:167–76.